**Automation and Machine Learning (2025)**
**Clausius Scientific Press, Canada**
**DOI: 10.23977/autml.2025.060103**
**ISSN 2516-5003 Vol. 6 Num. 1**

# *Design of a Passive Terahertz Real-time Imaging System Based on Microwave Kinetic Inductance Detectors (MKIDs)*

**Ning Dong**[1,a,*]
[1]*Industries Training Centre, Shenzhen Polytechnic University, Shenzhen, 518055, China*
[a]*dongning@szpu.edu.cn*
**Corresponding author*

***Keywords:*** MKID, Spatial Resolution, Terahertz Imaging

***Abstract:*** Terahertz imaging holds great potential in the field of security inspection. To meet this demand, this paper designs and constructs a passive terahertz real-time imaging system based on a MKID (Microwave Kinetic Inductance Detector) array and a spatial resolution layer. The system consists of an MKID detector array module, a spatial resolution layer module, a microwave signal coupling and amplification module, a signal mixing and acquisition module, an image reconstruction and processing module, a THz wave source and calibration module, a cryogenic superconducting module, and a microwave signal source and excitation module. Through the design of the MKID detector array, this paper enables the detection of the full frequency band of terahertz waves, significantly improving the sensitivity and accuracy of the detection system. By introducing the spatial resolution layer, spatial information is converted into time-domain signals, thus achieving spatial imaging of terahertz waves and enhancing the spatial resolution of the system. By adopting a digital acquisition system and fast signal processing algorithms, real-time acquisition and analysis of signals can be realized, further enhancing the real-time performance of the system.

## 1. Introduction

Security inspection, as a crucial part of the public safety field, plays an irreplaceable role in preventing extreme terrorist activities and stopping passengers from carrying prohibited and dangerous items. In crowded public gathering places such as airports, railway stations, and subways, it is particularly necessary to deploy security inspection equipment to conduct targeted inspections of people and items. With the emergence of terahertz superconducting detectors, long-distance passive THz real-time imaging technology has become a development direction of advanced security inspection technology due to its advantages such as comprehensive detection range, high speed, no blind spots in security inspection, and no invasion of personal privacy.

For long-distance passive THz real-time imaging, the self-radiation power of objects to be measured at room temperature is weak, which puts forward stringent requirements for the performance of detectors. That is, they need to have low noise and high sensitivity, and the noise equivalent power (NEP) needs to reach below the order of $10^{-14}$ W/Hz$^{1/2}$. Currently, only superconducting detectors operating at low temperatures can meet this specification [1]. The energy gap of superconducting materials is relatively small (~meV, 2 ~ 3 orders of magnitude lower than that of semiconductors). A photon with energy exceeding the energy gap can break up several Cooper pairs. Therefore, superconducting devices have an extremely wide response spectrum and can respond sensitively to photons from the visible light to the infrared and then to the THz band.

At present, the widely studied superconducting detectors mainly include three types: superconducting nanowire single photon detectors (SNSPD) [2], thermal sensitive superconducting edge sensors (TES) [3], and microwave kinetic inductance detectors (MKID) [4]. Among them, SNSPD detects photons by the loss of superconductivity in the hot-spot region formed when photons enter the nanowire. It has an extremely fast response speed and is mainly applied in the fields of quantum communication and optical quantum communication [5-7]. TES realizes photon detection by means of a superconducting thin-film with a very large slope of the superconducting transition curve. It has achieved certain application results in high-efficiency photon counting, photon energy resolution [8, 9], and passive imaging [10]. MKID, on the other hand, relies on the sensitive response of the kinetic inductance of superconducting materials to radiation energy for photon detection [11]. It is usually made into a superconducting resonator structure. When photons are absorbed, the resonant frequency and quality factor of the resonator will decrease. Compared with TES, MKID has the advantages of being relatively easy to fabricate, not requiring precise temperature control, and being more easily expandable into a large-scale array for reading. This makes it widely used in millimeter/sub-millimeter-wave astronomy imaging, such as the Balloon-Borne Large Aperture Submillimeter Telescope (BLAST) [12] in Antarctica, the Multi-band Unbiased Sub-millimeter Inductance Camera (MUSIC) [13], and the New IRAM KID Array (NIKA) [14] of the European millimeter-wave telescope project. It can be seen that the superconducting microwave kinetic inductance detector, with its low noise and easy expandability, has become one of the important ways to achieve high-sensitivity large-array $TH_2$ detectors and has broad application prospects.

This paper studies a high-performance terahertz (600GHz, 500um) superconducting MKID array imaging chip for human body security inspection, and combines a spatial resolution layer to construct a passive terahertz real-time imaging system, which can realize spatial real-time imaging including spectral information. The 600GHz frequency band is selected because it has good clothing penetration, a small air-propagation attenuation rate, and a high signal frequency. In fact, researchers from Cardiff University first demonstrated the application of MKID in passive TH imaging in 2016[15]. They fabricated a superconducting Al MKID array detector chip with 152 pixels, achieving a noise equivalent temperature difference (NETD) of approximately 0.1 K/Hz$^{1/2}$in the 350GHz detection frequency band, and the resolution for a target object 3-5m away is about 1.3cm. However, although existing technical solutions can detect THz light, there are obstacles in spatial imaging, making it difficult to effectively distinguish THz light from different spatial positions. When using an optical beam-splitting scheme for spatial resolution, there are problems such as slow speed and the inability to achieve single-shot imaging. The work of this paper, while retaining spectral information, fully balances the imaging resolution and imaging speed of the system, laying a foundation for further application in the security inspection field.

## 2. Experiment

### 2.1. Terahertz real-time imaging system

We designed and successfully constructed a terahertz real-time imaging system based on a Microwave Kinetic Inductance Detector (MKID) array and a spatial resolution layer, as shown in

Figure 1. This system integrates multiple key functional modules, and these modules work collaboratively to achieve efficient and accurate terahertz imaging.

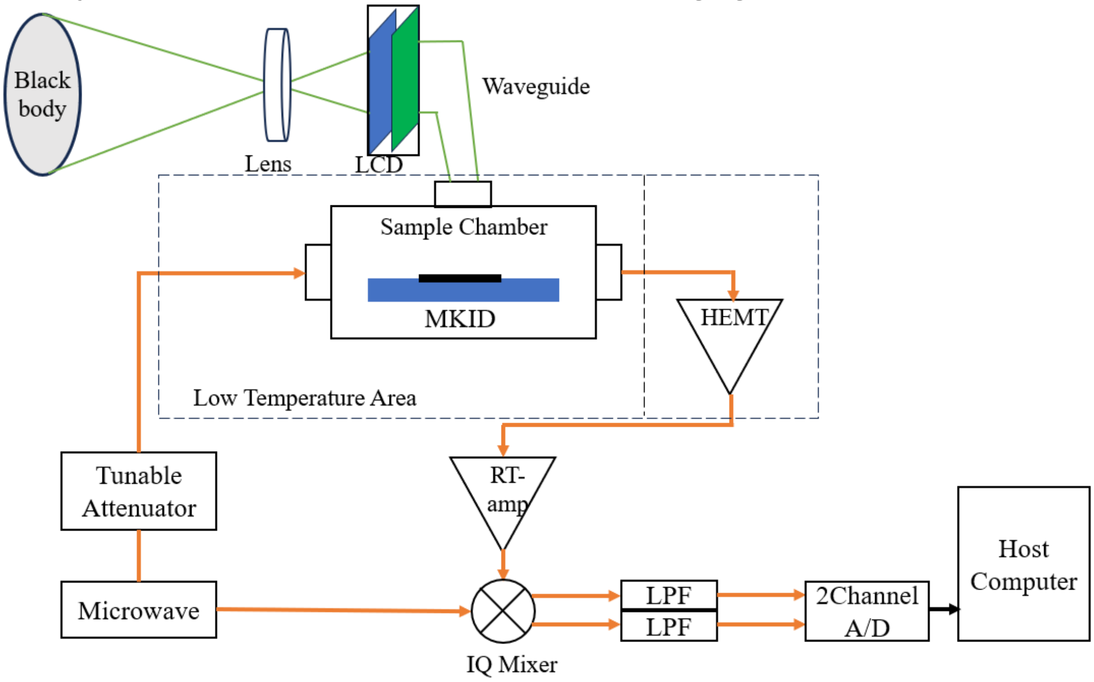


Figure 1. Schematic diagram of real-time imaging system

1) MKID Detector Array Module

This module is composed of multiple MKID pixels and has the ability to conduct high-sensitivity detection of the full frequency band of terahertz waves. Through the organic combination with the spatial resolution layer, based on the principle of time-resolved technology, high-resolution spatial imaging of the target is achieved.

2) Spatial Resolution Layer Module

This module adopts an innovative double-layer structure design of a liquid-crystal panel and a waveguide plate. By precisely regulating the terahertz signals at different spatial positions to pass through the liquid-crystal dots at specific times and efficiently transmit them to the MKID detector array, the spatial resolution function of the terahertz signals is realized, providing spatial information for subsequent imaging.

3) Microwave Signal Coupling and Amplification Module

Using a dedicated feeder, the weak microwave signals detected by the MKID detector array are transmitted to a cryogenic superconducting amplifier for preliminary amplification to enhance the signal strength. Subsequently, they are further processed by a room-temperature amplifier to meet the dynamic range requirements of signal processing, and then sent to a mixer for I/Q signal demodulation. Finally, a high-precision digital acquisition system is used to conduct a comprehensive time-domain analysis of the demodulated signals.

4) Signal Mixing and Acquisition Module

In this module, the input signal and the reference signal are precisely mixed in a mixer, generating an I-voltage output representing the signal amplitude information and a Q-voltage output representing the phase information. The mixed signal is filtered by a well-designed low-pass filter to remove high-frequency noise and then digitized and acquired through a high-performance A/D card to ensure the accuracy and reliability of the acquired signals.

5) Image Reconstruction and Processing Module

By applying time-domain signal processing algorithms, the time-domain microwave signals collected are deeply analyzed and processed. The information in different time dimensions is accurately extracted and integrated to reconstruct the terahertz spatial imaging.

6) THz Wave Source and Calibration Module

A temperature-controllable black-body source is used as the terahertz wave generation source. By controlling the temperature of the black-body source, stable and frequency-controllable terahertz waves are generated. The terahertz waves are filtered by a THz low-pass filter to remove clutter interference, and then the pure terahertz signals are transmitted to the MKID detector array in the sample box through a high-performance horn antenna for system calibration and imaging experiments, ensuring the accuracy and reliability of system imaging.

## 2.2. Spatial Resolution Layer

The spatial resolution layer adopts a double-layer structure design of a liquid-crystal panel and a waveguide plate. The working principle and signal transmission process are as follows:

As shown in Figure 2, the liquid-crystal panel precisely controls the light-transmittance state of each liquid-crystal dot through horizontal and vertical control lines according to preset rules. During the operation, each liquid-crystal dot sequentially changes to the light-transmittance state in a fixed order, enabling terahertz waves at different spatial positions to pass through the corresponding liquid-crystal dots. When terahertz waves are emitted from an external source and pass through the spatial resolution layer, each liquid-crystal dot gradually transmits signals from different spatial positions.

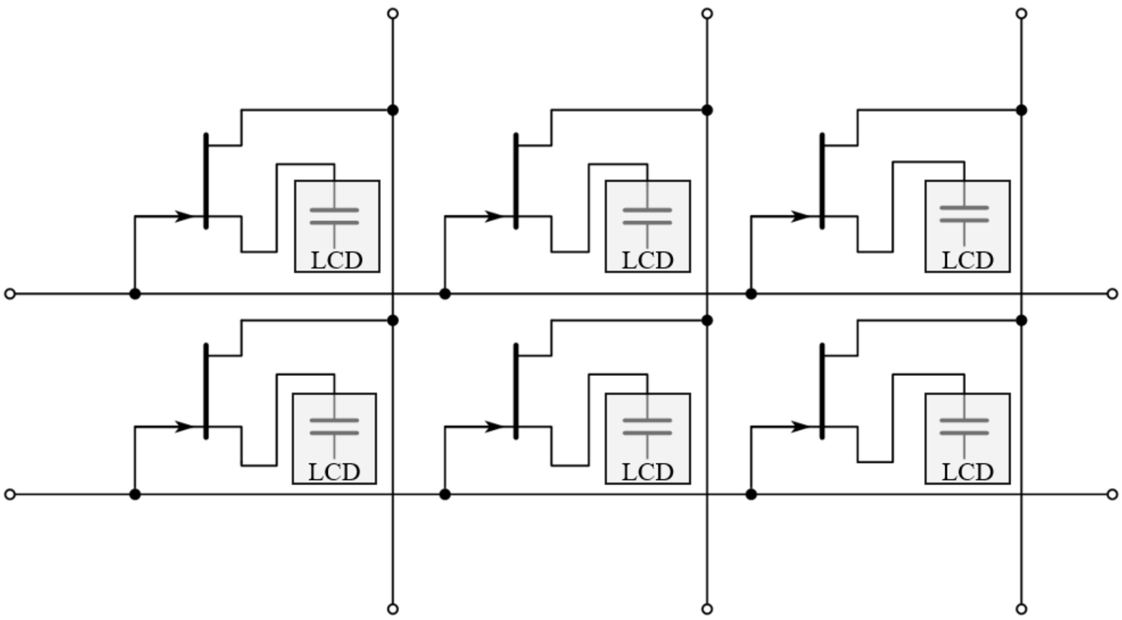


Figure 2. Liquid-crystal panel and its control circuit

Suppose the liquid-crystal panel contains $m \times n$ liquid-crystal pixels. The light-transmittance state of each pixel can be changed by controlling the voltage, and the refresh cycle of the liquid-crystal panel is $\delta t$. Its light-transmittance state can be accurately described by the following formula:

$$P(t) = \begin{cases} 1, & \text{light-transmissive} \\ 0, & \text{non-light-transmissive} \end{cases} \quad (1)$$

where $P(t)$ represents the light-transmittance state of the liquid-crystal pixel at time $t$, and $t$ is the time variable.

When a certain pixel on the liquid-crystal panel is in the open (light-transmissive) state, the terahertz signal can pass through this liquid-crystal dot and is transmitted to the MKID detector array by the waveguide plate. Let the transmission efficiency of the waveguide plate be $\eta_{wg}$, which is defined as the efficiency of the waveguide plate in successfully transmitting the terahertz signal passing through the liquid-crystal panel to the MKID array. Based on this, the signal transmission process can be expressed by the following formula:

$$S_{out}(t) = \eta_{wg} \cdot S_{in}(t) \cdot P(t) \tag{2}$$

where $S_{out}(t)$ is the terahertz signal transmitted to the MKID detector array, $S_{in}(t)$ is the incident signal transmitted through the liquid-crystal panel, $\eta_{wg}$ is the transmission efficiency of the waveguide plate, and $P(t)$ is the light-transmittance state of the liquid-crystal panel at time .

During the operation of the entire system, when a liquid-crystal pixel is opened, the terahertz wave signal from the corresponding spatial position will be transmitted to the corresponding pixel in the MKID detector array. Given that the refresh time of each liquid-crystal dot is $\delta t$, if the liquid-crystal panel has a total of $m \times n$ pixels and the refresh time of each pixel is $\delta t$ , then the refresh cycle of the entire panel can be expressed as:

$$T = m \times n \times \delta t \tag{3}$$

It can be seen that the time required to depict a complete image is the sum of the refresh times of $m \times n$ pixels.

## 3. Result Analysis

### 3.1. Theoretical Analysis

This section commences with a theoretical analysis of the factors influencing the spectral measurement and spatial resolution of terahertz imaging within the system.

#### 3.1.1. Microwave signal source and excitation module

The microwave signal source and excitation module serve to generate microwave signals, which are then transmitted to the MKID detector array via feeders. The excitation signal is designed to match the resonance frequency of the detector. When the detector receives terahertz photons, this matching excitation signal can trigger changes in the microwave signals.

When terahertz photons are absorbed by the detector, the carriers in the superconducting material are excited, leading to a change in its inductance. Since the frequency of the excitation signal is in tune with the resonant frequency of the detector, corresponding changes occur in the phase and amplitude of the microwave signal. By monitoring these changes in the microwave signal, data regarding terahertz photons can be obtained. Specifically, the changes in the phase and amplitude of the microwave signal can be represented by a complex number:

$$V(t) = A(t)e^{j(2\pi f t + \phi(t))} \tag{4}$$

where $V(t)$ is the voltage response of the microwave signal, $A(t)$ is the signal amplitude, $f$ is the signal frequency, and $\phi(t)$ is the signal phase.

As the number of absorbed photons increases, the change in current will cause a variation in the signal amplitude $A(t)$. The change in current also induces a change in the resonant frequency, which in turn leads to a change in the signal phase $\phi(t)$.

### 3.1.2. Microwave Signal Coupling and Amplification Module

The microwave signal coupling and amplification module is responsible for transmitting the detected microwave signals to a cryogenic superconducting amplifier through feeders. Subsequently, the signals are further processed by a room-temperature amplifier and then sent to a mixer for I/Q signal demodulation. Finally, a digital acquisition system is utilized for time-domain analysis.

The I and Q signals are digitized by an A/D converter (ADC). The ADC converts the analog signals into digital signals, enabling the signals to be processed and analyzed in subsequent digital signal processing. The digitized I/Q signals enter the digital signal processing system, where Fourier transform analysis is performed on the I/Q signals to obtain spectral information.

Specifically, further Fourier transform is carried out on the digitized I/Q signals to acquire the spectral information of the signals. The basic formula for the Fourier transform is as follows:

$$X(f) = \int_{-\infty}^{\infty} x(t)e^{-j2\pi ft}dt \quad (5)$$

where $x(t)$ is the time-domain signal, $X(f)$ is the frequency-domain signal.

For discrete digital I/Q signals, the Discrete Fourier Transform (DFT) is employed, and its formula is:

$$X[k] = \sum_{n=0}^{N-1} x[n]e^{-j\frac{2\pi}{N}kn} \quad (6)$$

where $N$ is the number of signal sampling points, $k$ is the frequency index, and $x[n]$ is the $n$-th sample of the signal in the time domain.

After the Fourier transform, the obtained spectral data represents the distribution of the signal in the frequency domain. Through visualization tools, the spectrogram can be plotted to examine the frequency characteristics of the signal.

Through spectral analysis, information such as the main frequency components, bandwidth, center frequency, and frequency offset of the signal can be extracted. Peak detection is performed on the spectrogram to identify specific frequency points of the signal, and further analysis of the signal properties is carried out. The center frequency of the signal is extracted from the spectrum to determine whether there is a frequency offset in the signal.

### 3.1.3. Signal Mixing and Acquisition Module

The signal mixing and acquisition module is designed to perform the mixing operation of the input signal and the reference signal within a mixer. Through this process, the I-voltage and Q-voltage outputs are obtained, which respectively represent the amplitude and phase information of the signal. Subsequently, the mixed-frequency signal undergoes low-pass filtering and is digitized and collected via an A/D card.

Preferably, in the mixer, the input signal $S(t)$ and the reference signal $LO(t)$ are subjected to a multiplication operation, resulting in the following mixing output:

$$S_{mix}(t) = S(t) \times LO(t) \quad (7)$$

Substituting the signal expressions:

$$S_{mix}(t) = A_S \cdot \cos(2\pi f_S t + \phi_S) \cdot A_{LO} \cdot \cos(2\pi f_{LO} t + \phi_{LO}) \quad (8)$$

using the trigonometric identity to expand the above-mentioned formula:

$$S_{mix}(t) = \frac{A_S A_{LO}}{2}\left[\cos\left(2\pi(f_S - f_{LO})t + (\phi_S - \phi_{LO})\right) + \cos(2\pi(f_S + f_{LO})t + (\phi_S + \phi_{LO}))\right] \quad (9)$$

The difference-frequency component is the desired low-frequency signal, which contains the amplitude and phase information of the signal; while the sum-frequency component is filtered out.

### 3.2. Analysis of imaging results

The performance of the THz spectral imaging system is critically dependent on the spatial resolution and imaging speed of the imaging. Similar to the traditional terahertz time-domain spectroscopy technology, a single-pixel terahertz imaging is achieved by using a MKID to scan and obtain the entire time-domain waveform, and then high-speed A/D is employed for data acquisition. Due to the extremely high sensitivity of the MKID, which can reach the single-photon level, it is capable of detecting signal changes in the picosecond (ps) magnitude, as shown in Figure 3(a). This high-sensitivity characteristic enables the system to capture subtle changes in the terahertz signals, contributing significantly to the accuracy and quality of the spectral imaging. It also provides a solid foundation for subsequent in-depth analysis of the spectral and spatial information of the detected objects.

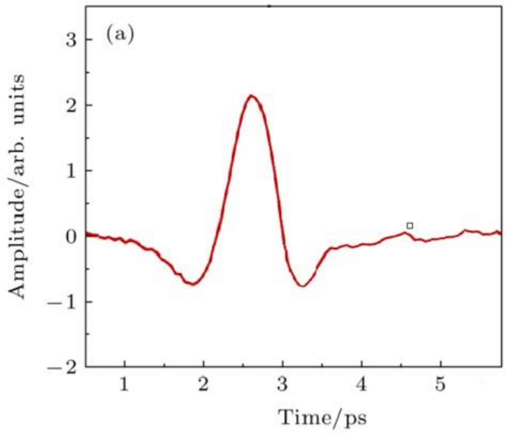


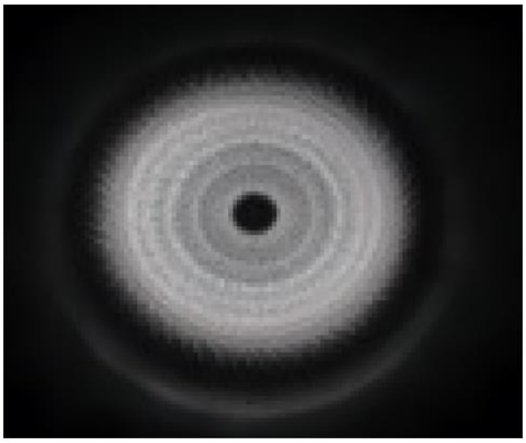


Figure 3. Analysis of imaging results. (a) The terahertz time domain waveform; (b) THz imaging of the perforated disk

Spatial imaging is then performed in combination with the spatially resolved layer. The imaging target is a perforated disk placed in a cryogenic environment of 3-11K, which can be approximated as a blackbody. This blackbody emits blackbody radiation in the range of 0.3-1THz. The terahertz waves are projected onto a controlled LCD array through a lens. Here, a 120×100 LCD array is adopted, and each pixel of the array is turned on one by one at time intervals of 100 microseconds, conducting spatial resolution in a point-by-point scanning manner. After an imaging time of approximately 1s, the terahertz image of the target can be obtained, as presented in Figure 3(a). This approach not only effectively utilizes the spatial resolution layer to achieve high-resolution spatial imaging but also takes full advantage of the high-sensitivity of the MKID detector, further enhancing the quality and detail-richness of the terahertz image.

## 4. Conclusions

This paper presents a passive terahertz real-time imaging system that combines a MKID detector with a spatial resolution layer. This system is capable of acquiring both the image information and spectral information of samples. Leveraging the high sensitivity of the MKID, it enables rapid measurement of weak terahertz light. Compared with traditional terahertz time-domain spectroscopy systems, it offers higher spatial resolution and faster imaging speed while preserving all spectral information. At a resolution of 120×100 pixels, a real-time frame rate of 1 f/s can preliminarily meet the application requirements in the security inspection field. Moreover, the full spectrum information can better distinguish the materials of objects. Additionally, this system also has excellent applications in fields such as non-destructive testing of materials, biological tissue analysis, and astronomy research. It has the potential to drive further development in the field of terahertz science and technology, opening up new possibilities for various applications that require high-resolution imaging and accurate spectral analysis.

## Acknowledgements

This article is an outcome of the project “Research and Fabrication of Superconducting Quantum Devices and Their Applications in Signal Detection” supported by “the Research Foundation of Shenzhen Polytechnic University under Grant 6023312035K”.

## References

*[1] Li, J., Zhang, W., Miao, W., & Shi, S. C. (2017). Development of Ultra-High Sensitivity Terahertz Superconducting Detection Technology. Chinese Optics (Chinese and English), 10(1), 122-130.*

*[2] C. Natarajan, M. G. Tanner, R. H. Hadfield, Superconducting nanowire single-photon detector systems for quantum optics applications, Superconductor Science and Technology, 25(6), 063001 (2012).*

*[3] A. J. Miller, S. W. Nam, J. M. Martinis, et al., Demonstration of a low-noise near-infrared photon counter with multiphoton discrimination, Applied Physics Letters, 83(4), 791-793 (2003).*

*[4] Zmuidzinas, J. (2012). Superconducting Microresonators: Physics and Applications. Annual Review of Condensed Matter Physics, 3(1), 169–198.*

*[5] Rosenberg, D., Nam, S., Hiskett, P., Nordholt, J., Peterson, C., & Hughes, R. (2006). Long-distance decoy-state quantum key distribution in optical fiber. Applied Physics Letters, 88(2), 021108.*

*[6] Sun, Q., Mao, Y., Chen, S., Xie, L., Zhou, H., & Duan, X. (2016). Giant nonlinear optical response in plasmonic nanostructures with quantum wells. Nature Photonics, 10(10), 671–676.*

*[7] Zhong, H., Wang, H., Deng, Y., Chen, M., Peng, L., Luo, Y., Qin, J., Wu, X., Li, S., Wang, Y., & Pan, J. (2020). Quantum computational advantage using photons. Science, 370(6523), 1460–1463.*

*[8] Lita, A. E., Miller, A. J., & Nam, S. W. (2008). Counting near-infrared single-photons with 95% efficiency. Optics Express, 16(5), 3032–3040.*

*[9] Fukuda, D., Fujii, G., Numata, T., Yoshizawa, A., Tsuchida, H., Fujino, H., Sato, H., Kirigaya, K., Yabuno, M., & Sasaki, M. (2011). High-efficiency superconducting single-photon detectors for near-infrared wavelengths. IEEE Transactions on Applied Superconductivity, 21(3), 241–244.*

*[10] Heinz, E., Müller, A., Schmidt, L., & Wagner, S. (2012). Development of Passive Submillimeter-Wave Video Imaging Systems for Security Applications. In Millimetre Wave and Terahertz Sensors and Technology V (Vol. 8544]). SPIE.*

*[11] Clem, J. R. (2013). Critical state in type-II superconductors with arbitrary cross-section and general longitudinal current. Journal of Applied Physics, 113(1), 013910.*

*[12] Galitzki, N., Ade, P., Angilè, F. E., Ashton, P., Beall, J., Becker, D., Bradford, K. J., Che, G., Cho, H.-M., Devlin, M., Dober, B., Fissel, L. M., Fukui, Y., Gao, J., Groppi, C., Hillbrand, S., Hilton, G., Hubmayr, J., Irwin, K., ... Zhu, N. (2014). The next-generation BLASTPol experiment. Journal of Astronomical Instrumentation, 3(2), 1440001.*

*[13] Say, J., Bock, C., Brug, S., Delderfield, J., Ferlet, M., & Ouaknine, J. (2014). The Sentinel-5 Precursor Instrument: Status and Performance of the UVNS Spectrometer. In Proceedings of SPIE: International Society for Optical Engineering (Vol. 9153, p. 915304). SPIE.*

*[14] Monfardini, A., Swenson, L. J., Bideaud, A., Benoit, A., Cruciani, A., Camus, P., Hoffmann, C., Desert, F. X., Doyle, S., Ade, P., Mauskopf, P., Tucker, C., & Roesch, M. (2010). A dual-band millimeter-wave kinetic inductance camera for the IRAM 30 m telescope. Astronomy & Astrophysics, 521, A29.*

*[15] Rowe, S., Pascale, E., Doyle, S., Brien, T., Hargrave, P., Mauskopf, P., & Ade, P. (2016). A scalable readout for microwave kinetic inductance detector arrays. Review of Scientific Instruments, 87(3), 033105.*